UCRL-PROC-214908

Water Under the Extreme Conditions of Planetary Interiors: Symmetric Hydrogen Bonding in the Superionic Phase

Nir Goldman, Laurence E. Fried

August 30, 2005

Americal Physical Society Topical Meeting on Shock
Conditions of Condensed Matter
Baltimore, CA, United States
July 31, 2005 through August 5, 2005

Water Under the Extreme Conditions of Planetary Interiors: Symmetric Hydrogen Bonding in the Superionic Phase

Nir Goldman* **and Laurence E. Fried**[†]

[*]7000 East Ave., L-268, Lawrence Livermore National Laboratory, Livermore, CA 94550
[†]L-282, LLNL, Livermore, CA 94550

Abstract. The predicted superionic phase of water is investigated via *ab initio* molecular dynamics at densities of 2.0-3.0 g/cc (34 -115 GPa) along the 2000K isotherm. We find that extremely rapid (superionic) diffusion of protons occurs in a fluid phase at pressures between 34 and 58 GPa. A transition to a stable body-centered cubic (bcc) O lattice with superionic proton conductivity is observed between 70 and 75 GPa, a much higher pressure than suggested in prior work. We find that all molecular species at pressures greater than 75 GPa are too short lived to be classified as bound states. Above 95 GPa, a transient network phase is found characterized by symmetric O-H hydrogen bonding with nearly 50% covalent character.

Keywords: superionic, water, ab initio, molecular dynamics, planetary interiors
PACS: 61.20Ja, 31.15Ar, 71.15Pd, 62.50+p

INTRODUCTION

The density profiles of large planets, such as Uranus and Neptune, suggest that there exists within a thick layer of “hot ice”, which is thought to be 56% H_2O, 36% CH_4, and 8% NH_3[1]. This has lead to a theoretical prediction of a superionic phase of water[2, 3], wherein the oxygen atoms have formed a bcc lattice, and the hydrogens diffuse at rates comparable that of the ambient liquid. However, these results have been controversial, both in terms of theory[4] and experiment[5, 6, 7]. Here, we investigate the hot, compressed phase of water with extensive first principles Car-Parrinello molecular dynamics simulations, the results of which have been published previously[8]. Calculated power spectra (i. e., the vibrational density of states, or VDOS) have recently been compared to measured experimental Raman spectra[9] at pressures up to 55 GPa and temperatures of 1500K. The agreement between theory and experiment was very good. In particular, weakening and broadening of the OH stretch mode at 55 GPa was found both theoretically and experimentally.

It is the goal of this work to re-evaluate the phase diagram of water by characterizing the superionic phase in terms of its structure, dynamics, and molecular composition. In the present study, we focus our efforts on an area of the phase diagram that is likely to show a transition to the superionic phase. We report results of simulations along the 2000K isotherm, at pressures of 34 – 115 GPa (2.0 – 3.0 g/cc).

COMPUTATIONAL DETAILS

For our simulations, we used the CPMD code v.3.91, with the BLYP exchange-correlation functional[10, 11], and Troullier-Martins pseudo-potentials[12] for both oxygen and hydrogen. A planewave cutoff of 120 Ry was employed to insure convergence of the pressure, although all other properties were seen to converge with a much lower cutoff (85 Ry). The system size was 54 H_2O molecules. The temperature was controlled by using Nosé-Hoover thermostats[13] for all nuclear degrees of freedom. The importance of an appropriate choice of electron mass in Car-Parrinello molecular dynamics of water has been pointed out in recent studies[14, 15]. We chose a conservative value of 200 au, and a time step of 0.048 fs. Initial conditions were generated in two ways: 1) a liquid configuration at 2000K was compressed from 1.0 g/cc to the desired density in sequential steps of 0.2 g/cc from an equilibrated sample. 2) An ice VII configuration was relaxed at the density of interest, then heated to 2000K in steps of 300 degrees each for a duration of 0.5 – 1 ps. While heating the temperature was controlled via velocity scaling. We will refer to the first set of simulations as the “L” set, and the second as the “S” set. Unless stated otherwise, the results (including the pressures) from the “S” initial configurations are those reported. Once the desired density and/or temperature were achieved, all simulations were equilibrated for a minimum of 2 ps. Data collection simulations were run from 5–10 ps.

DYNAMICS AND STRUCTURE

The calculated diffusion constants for both "L" and "S" simulations are virtually identical up until 2.6 g/cc. At 34 GPa (2.0 g/cc), the hydrogen atom diffusion constant has achieved values associated with superionic conductivity (greater than $10^{-4}\text{cm}^2/\text{s}$). The diffusion constant remains relatively constant with increasing density, in qualitative agreement with the experimental results of Chau et al.[6] for the ionic conductivity. On the other hand, the O diffusion constant drops to zero at 75 GPa (2.6 g/cc) for both “L” and “S” initial configurations. The surprisingly small hysteresis in the fluid to superionic transition allows us to place the transition point between 70 GPa (2.5 g/cc) and 75 GPa (2.6 g/cc).

All radial distribution functions (RDF) for the "S" simulations are shown in Figure 1. Analysis of the oxygen-oxygen RDF for all pressures yields a coordination number of the first peak of just over 14, consistent with a high density bcc lattice in which the first two peaks are broadened due to thermal fluctuations. The RDF was further analyzed by calculating an “average position” RDF in which the position of each oxygen was averaged over the course of the trajectory. The results for 75 – 115 GPa indicate the presence of bcc lattice undergoing large amplitude vibrations, even though the RDF’s have width similar to that of a liquid or a glass. The RDFs for the amorphous phase are similar to those of the solid phase obtained in the “S” simulations.

The O–O and H–H RDFs indicate that no O-O or H-H covalent bonds are formed during the simulations at all densities. The $g(R_{OH})$ shows a lattice-like structure at 115 GPa, which is consistent with proton diffusion via a hopping mechanism between lattice sites[3]. At 34 GPa, the coordination number for the first peak in $g(R_{OH})$ is 2, indicating molecular H_2O. At 95 – 115 GPa, however, the coordination number for the first peak in $g(R_{OH})$ becomes 4, indicating that water has formed symmetric hydrogen bonds where each oxygen has four nearest neighbor hydrogens.

Concomitant with this is a shift of the first minimum of the O–H RDF from 1.30Å at 34 GPa to 1.70Å at 115 GPa. We observe a similar structural change in the H–H RDF in which the first peak lengthens from 1.63Å (close to the result for ambient conditions) to 1.85Å . These observations bear a strong resemblance to the ice VII to ice X transition in which the covalent O–H bond distance of ice becomes equivalent to the hydrogen bond distance as pressure is increased[16]. However, the superionic phase differs from ice X, in that the position of the first peak in $g(R_{OH})$ is not half the distance of the first O-O peak[16]. We analyze the effect of the change in $g(R_{OH})$ below in terms of the molecular speciation in the simulations.

FREE ENERGY BARRIER AND CHEMICAL SPECIES

We have determined the free energy barrier for dissociation by defining a free energy surface for the oxygen-hydrogen distances, viz. $W(r) = -k_B T \ln[g(R_{OH})]$, where $W(r)$ is the free energy surface (potential of mean force). The results are shown in Figure 2. We define instantaneous species based on the O–H bond distance. If the bond distance is less than a value r_c, we count the atom pair as bonded. Determining all the bonds in the system gives the chemical species at each point in time. Species with lifetimes less than an O–H bond vibrational period (10 fs) are “transient”, and do not represent bound molecules. The optimal cutoff r_c between bonded and non-bonded species is given

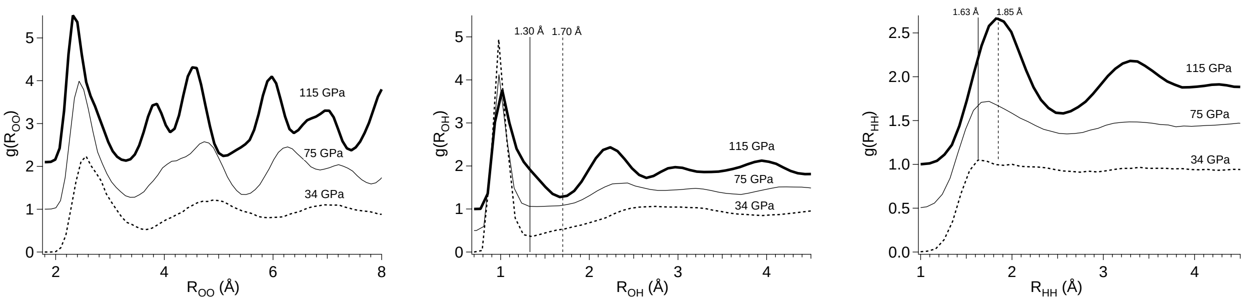

FIGURE 1. Radial distribution functions as a function of density. At 34 GPa we find a fluid state. At 75 GPa we show a "covalent" solid phase. At 115 GPa, we find a "network" phase with symmetric hydrogen bonding. Structural changes in the O-H and H-H RDFs are highlighted in the figure.

by the location of the maximum in the free energy surface[17].

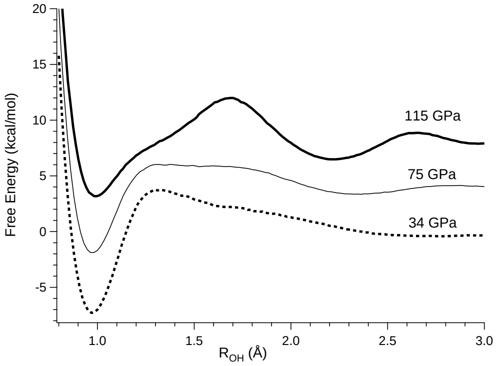

FIGURE 2. R_{OH} free energy surface. The lines are spaced by a factor of 4 kcal/mol for clarity.

The use of the free energy maximum to define a bond cutoff provides a clear picture of qualitative trends. As expected from the $g(R_{OH})$, at 34 GPa, the free energy peak is found at 1.30Å, which is approximately the same value obtained from simulations of ambient water. At 75 GPa, the free energy peak maintains almost the same position, but broadens considerably. At 115 GPa, the peak has sharpened once again, and the maximum has increased dramatically to 1.70Å.

Given the above definition of a bond distance, we have analyzed species lifetimes. Above 2.6 g/cc, the lifetime of all species is less than 12 fs, which is roughly the period of an O-H bond vibration (ca. 10 fs). Hence, water above 75 GPa and at 2000K does not contain any molecular states, but instead forms a collection of short-lived "transient" states. The "L" simulations at 2.6 g/cc (77 GPa) and 2000K yield lifetimes nearly identical to that found in the "S" simulations described above (within 0.5 fs). This indicates that the amorphous states formed from the "L" simulations are closely related to the superionic bcc crystal states found in the "S" simulations.

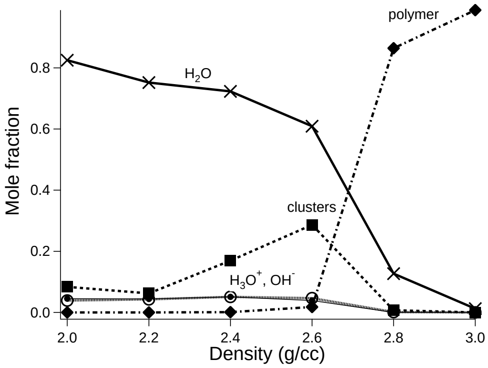

FIGURE 3. Mole fraction of species found at 34 – 115 GPa. The filled circles correspond to H_3O^+, while the open circles to OH^-.

Species concentrations were calculated for all simulations (Figure 3). At 34 GPa (2.0 g/cc), H_2O is the predominant species, with H_3O^+ and OH^- having mole fractions of ca. 5%. In addition, some aggregation has occurred in which neutral and ionic clusters containing up to six oxygens have formed. The concentrations of OH^- and H_3O^+ is low for all densities investigated, and non-existent at 95 and 115 GPa (2.8 and 3.0 g/cc). The calculated lifetimes for these species is well below 10 fs for the same thermodynamic conditions (less than 8 fs at 34 GPa). At pressures of 95 and 115 GPa, the increase in the O-

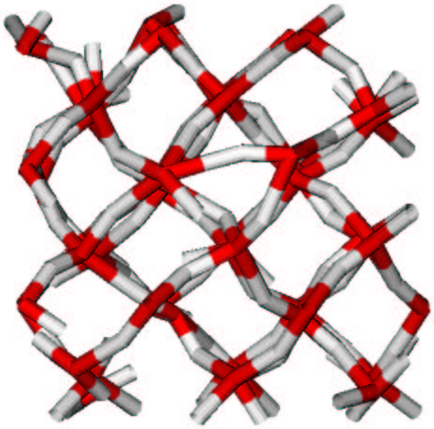

FIGURE 4. A snapshots of the simulations at 115 GPa. The protons dissociate very rapidly and form networks of bonds.

H bond distance leads to the formation of extensive bond networks (Figure 4). These networks consist entirely of O–H bonds, while O–O and H–H bonds were not found to be present at any point.

DISCUSSION

We have performed first principles simulations of water at pressures up to 115 GPa (3.0 g/cc) and 2000K. Along this isotherm we can define three different phases. First, from 34 GPa to 58 GPa (2.0-2.4 g/cc), we observe a molecular fluid phase with superionic diffusion of the hydrogens. Second, at 75 GPa (2.6 g/cc), we find a stable bcc oxygen lattice with superionic proton conduction. O–H bonds within this "solid" phase are found to be mostly covalent, despite their exceedingly short lifetimes of ca. 10 fs. Third, at 95 – 115 GPa (2.8 – 3.0 g/cc) we find a transformation to a phase dominated by transient networks of symmetric O-H hydrogen bonds. Given the smooth nature of the calculated P-V isotherm[8], the transition to the network phase does not appear to be first order. The network can be attributed to the symmetrization of the hydrogen bond, similar to the ice VII to ice X transition.

ACKNOWLEDGMENTS

This work was performed under the auspices of the U. S. Department of Energy by the University of California Lawrence Livermore National Laboratory under contract No. W-7405-Eng-48. We thank Alex Goncharov for a critical reading of the manuscript.

REFERENCES

1. Hubbard, W. B., *Science*, **214**, 145 (1981).
2. Demontis, P., LeSar, R., and Klein, M. L., *Phys. Rev. Lett.*, **60**, 2284 (1988).
3. Cavazzoni, C., Chiarotti, G. L., Scandolo, S., Tosatti, E., Bernasconi, M., and Parrinello, M., *Science*, **283**, 44–46 (1999).
4. Schwegler, E., Galli, G., Gygi, F., and Hood, R. Q., *Phys. Rev. Lett.*, **87**, 265501–1 (2001).
5. Nellis, W. J., Holmes, N. C., Mitchell, A. C., Hamilton, D. C., and Nicol, M., *J. Chem. Phys*, **107**, 9096–9100 (1997).
6. Chau, R., Mitchell, A. C., Minich, R. W., and Nellis, W. J., *J. Chem. Phys*, **114**, 1361 – 1365 (2001).
7. Katoh, E., Yamawaki, H., Fujihisa, H., Sakashita, M., and Aoki, K., *Science*, **295**, 1264 (2004).
8. Goldman, N., Fried, L. E., Kuo, I.-F. W., and Mundy, C. J., *Phys. Rev. Lett.*, **94**, 217801 (2005).
9. Goncharov, A. F., Goldman, N., Fried, L. E., Crowhurst, J. C., Kuo, I.-F. W., Mundy, C. J., and Zaug, J. M., *Phys. Rev. Lett.*, **94**, 125508 (2005).
10. Becke, A. D., *Phys. Rev. A*, **38**, 3098 (1988).
11. Lee, C., Yang, W., and Parr, R. G., *Phys. Rev. B*, **37**, 785 (1988).
12. Troullier, N., and Martins, J., *Phys. Rev. B*, **43**, 1993 (1991).
13. Hoover, W. G., *Phys. Rev. A*, **31**, 1695 (1985).
14. Grossman, J., Schwegler, E., Draeger, E. W., Gygi, F., and Galli, G., *J. Chem. Phys.*, **120**, 300–311 (2004).
15. Kuo, I.-F., Mundy, C., McGrath, M., Siepmann, J., VandeVondele, J., Sprik, M., Hutter, J., Chen, B., Klein, M., Mohamed, F., Krack, M., and Parrinello, M., *J. Phys. Chem. B*, **108**, 12990–12998 (2004).
16. Benoit, M., Romero, A. H., and Marx, D., *Phys. Rev. Lett.*, **89**, 145501–1 (2002).
17. Chandler, D., *J. Chem. Phys.*, **68**, 2959–2970 (1978).